

## Evaluation of uncertainty in flow and performance parameters in Francis turbine test rig

Ali Abbas<sup>a,b,\*</sup>, Arun Kumar<sup>a</sup>

<sup>a</sup> Alternate Hydro Energy Centre, Indian Institute of Technology Roorkee, Roorkee 247667, India

<sup>b</sup> Research Associate, at Alternate Hydro Energy Centre, IIT Roorkee



### ARTICLE INFO

#### Keywords:

In-situ calibration  
Uncertainty  
Flow calibration

### ABSTRACT

Model tests on hydraulic turbine are essential in hydraulic turbine development and related fields. The methods and technologies used to perform these tests show a constant progress. In addition, due to contractual nature, the demand for model test of turbines is increasing continuously in terms of quantity and accuracy. In this study, in situ calibration of different measuring instruments used in turbine model testing viz. flow meter, measuring tank load cells, calibrator tank load cell, shaft torque transducer, friction torque load cell and speed transducer have been performed and calibration equations have been derived from their calibration curves. The gravimetric approach using the flying start and stop method has been adopted for flow calibration in present study. Type A and Type B uncertainties of weighing balance and flow diverter has been evaluated as per ISO 4185:1980 [5] and JCGM 100: 2008 [13]. As per IEC 60193:1999 [3] performance test on the model has been conducted and efficiency as well as others flow parameters viz. discharge, head, speed and torque have been obtained at 16 different operating points including finding out Type A uncertainty in efficiency measurement. At each operating point, the regression error, Type A and Type B uncertainties are calculated in order to find out total uncertainty of flow and performance parameters. The total uncertainty in flow measurement and efficiency measurement at

**Abbreviations:** n, Number of observation;  $s(x_i)$ , Standard deviation of the mean value ( $x_i$ );  $P_m$ , Mechanical power from the turbine [W];  $P_h$ , Available hydraulic power [W];  $H$ , Net head [m]; BEP, Best efficiency point; PL, Part load; OL, Over load;  $Q_{wd}$ , Discharge coefficient;  $E_{wd}$ , Energy coefficient; ISO, International organization for standardization;  $(W_{CT})_C$ , Calibrated value of weight calibration tank [kg];  $(mV)_{CT}$ , measured voltage by calibrator tank load cell [mV]; SCADA, Supervisory control and data acquisition;  $Q_C$ , Calibrated discharge [ $m^3/s$ ];  $F_F$ , Frequency obtained from flow meter [kHz];  $(W_{MT})_C$ , calibrated value of weight by measuring tank [N-m];  $(mV)_{MT}$ , measured voltage by measuring tank load cell [mV];  $ST_C$ , calibrated value of shaft torque [N-m];  $F_{ST}$ , frequency obtained from shaft torque sensor [kHz];  $(RPM)_C$ , calibrated speed of turbine [1/min];  $(RPM)_M$ , Measured rpm by speed sensor [1/min];  $P_C$ , calibrated differential pressure [kPa];  $P_M$ , measured pressure from differential pressure [kPa];  $W_C$ , calibrated friction load weight [kg];  $W_M$ , measured friction [kg];  $u(Q)_a$ , Type A uncertainty of discharge measurement;  $u(Q)_b$ , Type B uncertainty of discharge measurement;  $u(wb)$ , uncertainty due to the weighing machine;  $u(p)$ , uncertainty due to diverter system;  $u(t)$ , uncertainty due to the timing device;  $u(\epsilon)$ , uncertainty due to buoyancy;  $M$ , true mass [kg];  $W$ , measured weight by load Cell [kg];  $\rho_{air}$ , density of air [ $kg/m^3$ ];  $\rho_f$ , density of the fluid (water) [ $kg/m^3$ ];  $\rho_w$ , density of the tank material [ $kg/m^3$ ];  $u(wb)_c$ , combined uncertainty of weighing balance system;  $u(wb)_a$ , type A uncertainty of weighing balance system;  $u(wb)_b$ , type B uncertainty of weighing balance system;  $\delta m_1$ , Error in mass determination of water in measuring tank before diversion;  $\delta m_2$ , Error in mass determination of water in measuring tank after diversion;  $\delta(\Delta m)$ , Uncertainty in mass of water collected in measuring tank;  $u(p)_c$ , combined standard uncertainty of the diverter system;  $u(p)_a$ , Type A uncertainty of the diverter system;  $u(p)_b$ , Type B uncertainty of the diverter system;  $\Delta t$ , Correction time [s];  $u(t)$ , Standard uncertainty of the timer [%];  $u(p)$ , Standard uncertainty of the diverter [%];  $u(d)$ , Standard uncertainty of the density [%];  $u(Q)_b$ , Type B uncertainty of the discharge measurement [%];  $u(Q)_a$ , Type A uncertainty of the discharge measurement [%];  $u(Q)_{reg}$ , Regression uncertainty of the discharge measurement [%];  $u(Q)_c$ , Combined uncertainty of the discharge measurement [%];  $u(Q)$ , Expanded uncertainty of the discharge measurement [%];  $u(T)$ , total torque uncertainty [%];  $u(ST)$ , shaft torque uncertainty [%];  $u(FT)$ , friction torque uncertainty [%];  $u(ST)_c$ , Combined uncertainty of the Shaft torque [%];  $u(ST)_a$ , Type A uncertainty of the Shaft torque [%];  $u(ST)_b$ , Type B uncertainty of the Shaft torque [%];  $u(ST)_{reg}$ , regression error at nearest operating point;  $u(w, st)$ , combined uncertainty of weight used for calibration [%];  $u(cal, arm)$ , uncertainty in measurement of calibration arm [%];  $u(FT)_a$ , Type A uncertainty of the friction torque [%];  $u(FT)_b$ , Type B uncertainty of the friction torque [%];  $v_1$ , uncertainty of inlet velocity [%];  $v_2$ , uncertainty of outlet velocity [%];  $(\Delta p)/\rho * g$ , differential head [m];  $(v_2/1-v_2/2/2 * g)$ , dynamic head [m];  $u(\eta)$ , uncertainty of efficiency measurement [%];  $u(T)$ , uncertainty in torque measurement [%];  $u(H)$ , uncertainty in head measurement [%];  $u(d)$ , uncertainty in density measurement [%];  $u(\omega)$ , Uncertainty in angular speed measurement of model turbine [%];  $u(\eta)_a$ , Type A uncertainty of efficiency measurement [%];  $u(\eta)_b$ , Type B uncertainty of efficiency measurement [%];  $u(\eta)_c$ , Combined uncertainty of efficiency measurement [%]

\* Corresponding author at: Alternate Hydro Energy Centre, Indian Institute of Technology Roorkee, Roorkee 247667, India.

E-mail address: [abbas.abbas02@gmail.com](mailto:abbas.abbas02@gmail.com) (A. Abbas).

<https://doi.org/10.1016/j.flowmeasinst.2019.01.009>

Received 14 July 2017; Received in revised form 1 December 2018; Accepted 6 January 2019

Available online 08 January 2019

0955-5986/© 2019 Elsevier Ltd. All rights reserved.

the best efficiency point has been found out minimum when compared with other operating points. In this paper, a correlation for the estimation of uncertainty in the efficiency measurement has been developed with an error of  $\pm 9\%$ .

## 1. Introduction

The main aim of the hydraulic turbine model tests is the prediction of hydraulic performances in terms of power output and efficiency. Nowadays, the most of the contracts specify performance guarantees in the order of 0.01% and high penalties from a 0.1% deviation between specifications and actual performance [1]. Any test, be it in a laboratory or in the field, is subject to the experimental errors and uncertainties. In the recent years, measurement accuracy has been improved by using electronic transducers, data acquisition system and high-speed integration techniques associated with computerized analysis of electronic signals. Instruments with the claim of 0.05% or less accuracy are available for measuring major parameters viz. head, power, discharge and speed. Fast-response instruments can record high-speed hydraulic parameters and integrate them to obtain extremely precise average values of the measured parameters and the calculated efficiencies [2].

### 1.1. Types of uncertainty

The range within which the true value of a measured quantity can be expected to lie, with a suitably high probability, is termed as uncertainty in measurement. Given the same type of probability distribution (95%confidence limit) of the Type A and Type B, the total uncertainty is combined by the root-sum-square method. There are three types of error/uncertainties that arise in the measurements as follows:

#### 1.1.1. Spurious errors

These are errors such as human errors, or instrument malfunction, which invalidate a measurement. For example, the presence of pockets of air in the pipe line connected to pressure transducer. Such errors are not incorporated into any statistical analysis and hence are discarded.

#### 1.1.2. Type A uncertainty

Type ‘A’ evaluation of standard uncertainty applies to the situation when several independent observations have been made for any of the input quantities under the same conditions of measurement. If there is sufficient resolution in the measurement process, there will be an observable scatter or spread in the value obtained. Whilst no correction can be made to remove random components of uncertainty, their

associated uncertainty becomes less as the number of observation/measurement increases. The measurements deviate from their mean in accordance with the laws of chance, such that their distribution usually approaches a normal distribution as the number of measurements is increased [3].

The standard Type A uncertainty of the mean value can be calculated by the Eq. (1)

$$U(\bar{x}_i) = \frac{s(x_i)}{\sqrt{n}} \tag{1}$$

where, n is the number of observation;  $s(x_i)$  is the standard deviation of the mean value ( $x_i$ ) can be calculated accordance with Eq. (2)

$$s(x_i) = \sqrt{\frac{1}{(n - 1)} \sum_{m=1}^n (x_{i,m} - \bar{x}_i)^2} \tag{2}$$

#### 1.1.3. Type B uncertainty

Type B elevation of uncertainty is those carried out by means other than the statistical analysis of series of observation/measurement. Therefore it cannot be reduced by increasing the number of measurements if the equipment and conditions of measurements remain unchanged. The associated estimated the standard uncertainty is evaluated by scientific judgment based on all of the available information on the possible variability. It includes the following information i.e. (a) Previous measurement data; (b) Experience with or general knowledge of the behavior and properties of relevant materials and instruments; (c) Manufacturer's specifications; (d) Data provided in calibration and other certificates.

To carry out the performance test, model test laboratories generally follow guideline available in IEC 60193:1999 [3], ASME PTC 18-2011 [4] and ISO 4185:1980 [5] for instrumentation, calibration, measurements procedure, data analysis and uncertainty evaluation of flow and performance parameters. Expected uncertainty of flow and performance parameters are presented in Table 1 as per as IEC-60193:1999 [3] and ISO 4185:1980 [5].

Only few researchers have shown interest in the uncertainty measurement of different flow and performance parameters due to requirement of complex and expensive experimental set up in order to meet out the standard provided in IEC 60193:1999 [3], ASME PTC 18-2011 [4] and ISO 4185:1980 [5].

**Table 1**  
Expected uncertainty of flow and performance parameters [3–5].

S. no.	Parameter	Method	Expected uncertainty	Component and expected uncertainty	
1.	Discharge	Flying start and stop with Weighing method	$\pm 0.1\%$ to $\pm 0.2\%$ (Systematic)	Diverter	Systematic $\leq 0.05\%$ Random $\leq 0.1\%$
				Weighing balance	Systematic $\leq 0.05\%$ Random $\leq 0.1\%$
				Timer	Systematic $\leq 0.01\%$
				Density	Systematic $\leq 0.05\%$
				Buoyancy	Systematic $\leq 0.01\%$
2.	Torque	Primary method	$\pm 0.15\text{--}0.25\%$ (Systematic)	Shaft torque	Systematic: $\pm 0.15\text{--}0.25\%$
				Friction torque	Systematic $\pm 0.02\text{--}0.05\%$ , of max torque
3.	Net head	–	$\pm 0.1\text{--}0.2\%$ (Systematic)	Pressure transducer	$\pm (1 - 5) \times 10^{-3} p_{max}^2$
				Free water level (ultrasonic)	$\pm 0.002\text{ m to } \pm 0.010\text{ m}$
4.	Speed	–	$\pm 0.01\text{--}0.05\%$ (Systematic)	–	–
5.	Efficiency (at BEP)	–	Random $\leq 0.1\%$ Total $\leq 0.25\%$	–	–

Stople and Fjærvold [6,7] performed the efficiency test on a Kaplan turbine at, Water Power laboratory, NTNU, Norway. Measurements were performed for two different blade angle settings although complete test could not be conducted. It was concluded that even though efficiency is reasonably high but the measurements has high uncertainties in efficiency as much as ± 1.58% [6,7]. The rig was re-developed by Kvangernes [8] and efficiency test of the same model was performed for wide operating range. Random and systematic uncertainty of different flow and performance parameters at the best efficiency point (BEP) for two different blade angle setting were reported as shown in Table 2.

The measurements of flow and performance parameters with uncertainty evaluation were conducted in the same laboratory on a reduced-scale (1:5.1) model of the prototype Francis turbines operating at the Tokke power plant, Norway. IEC 60193:1999 [3] was followed for the calibration, measurements, and computations of the data. Uncertainties in the discharge, inlet pressure, and differential pressure measurements were ± 0.1%, ± 0.05%, and ± 0.018%, respectively. The uncertainties in the generator input torque measurement, friction torque measurement, and runner angular speed measurement were ± 0.034%, ± 0.052, and ± 0.05%, respectively. Total uncertainty in the hydraulic efficiency was ± 0.16% under the steady-state operating condition of best efficiency point [9,10].

Performance test were conducted [11] on Turbine-99 Kaplan model consists of a 1:11 scale copy of the Hölleforsen power station, at the Vattenfall Turbine test rig, Sweden as per IEC 60193:1999 [3]. Uncertainty in the flow rate measurement and efficiency were reported as ± 0.13% and ± 0.20% respectively [11].

Andersson and Cervantes [11] used IEC 60193:1999 [3] to estimate the random errors, systematic errors, and other uncertainties. for the systematic uncertainties in the discharge, rotational speed, torque, and water head are ± 0.188%, ± 0.025%, ± 0.075%, and ± 0.065%, respectively, which corresponds to a ± 0.214% systematic uncertainties in the hydraulic efficiency calculated. The random uncertainty toward the hydraulic efficiency was estimated to a band of ± 0.10% by several measurements of mean value and standard deviation [12].

## 2. Experimental set up and calibration system

A model on scaled down level of 1:12.52 of a prototype Francis turbine having specification head as 27.432 m, power as 45 MW, runner diameter as 3.9881 m, discharge as 141.58 m<sup>3</sup>/s and speed as 112.5 rpm has been selected for the present investigations. The model turbine is investigated at the Hydraulic Turbine R&D Laboratory, AHCC, IIT Roorkee, India. A three dimensional view of test rig is presented as Fig. 1.

Water is circulated in the closed loop and pumped to the high pressure tank connected to the turbine from where it flows to the low pressure tank open to the atmosphere and released back to suction of

pump. The turbine model is integrated with 10 stay vanes conjoined inside the spiral casing, 20 guide vanes, runner with 15 blades, and an elbow-type draft tube. An electro-magnetic flow meter (ABB-FEP/13E/32) is used to measure the turbine discharge and a differential pressure transducer (Yokogawa-EJX110A) is used to acquire the pressure difference across the turbine. A non-contact type torque meter (HBM-T12) is used to measure the main torque along with load cell (HBM-Z6) used to measure the friction torque in hydro static bearing. The flow and operating parameters such as discharge, turbine inlet and differential pressure, atmospheric pressure, the angular speed of the runner, shaft torque to the generator, the bearing friction torque, the turbine axial force, and the guide vanes angular position were acquired through the SCADA system (Rockwell automation) with 100 Hz sample rate.

The hydraulic efficiency is defined as the output mechanical power ( $P_m$ ) from the turbine, relative to the available hydraulic power ( $P_h$ ). The output mechanical power ( $P_m$ ) and available hydraulic power ( $P_h$ ) are expressed by Eqs. (3) and (4) respectively. Net head ( $H$ ) is derived by Bernoulli's equation as given in Eq. (5).

Dimensionless parameters i. e discharge coefficient ( $Q_{\omega d}$ ) and energy coefficient ( $E_{\omega d}$ ) can be defined as given in Eqs. (6) and (7) respectively.

$$P_m = T^*\omega : \text{where, } \omega = \frac{2^*\pi^*N}{60} \tag{3}$$

$$P_h = \rho^*Q^*g^*H \tag{4}$$

$$H = \frac{(\Delta p)}{\rho^*g} + \frac{(v_1^2 - v_2^2)}{2^*g} \tag{5}$$

where, indexes 1 and 2 represents the system inlet and outlet, respectively.

$$E_{\omega d} = \frac{g^*H}{\omega_m^2*d^2} \tag{6}$$

$$Q_{\omega d} = \frac{Q}{\omega_m*d^3} \tag{7}$$

Performance test were conducted at a fixed model speed of 1000 rpm and a fixed energy coefficient ( $E_{\omega d} = 0.1723$ ) by varying the guide vane opening at four different operating points: best efficiency point (BEP), overload (OL) and two part load points (PL<sub>1</sub> and PL<sub>2</sub>) corresponding to 0.169, 0.1852, 0.1516 and 0.1181 discharge coefficient  $Q_{\omega d}$  values respectively. These tests were repeated at three others energy coefficient  $E_{\omega d}$  values of 0.1421, 0.1353 and 0.1285.

### 2.1. Head measurement system and calibration

Differential pressure transducers are installed in the head measurement panel as shown in Fig. 2.

A known amount of pressure taken from the nitrogen gas as the source is applied through pressure calibrator (Fluke-PPC4) to pressure

**Table 2**  
Uncertainty of parameters at BEP [8].

Parameters	Operating point	Measurement uncertainty resulting from unknown systematic deviations (%)	Random uncertainty (%)	Total uncertainty (%)
Torque	BEP for setting 1	0.2974	0.0048	0.2974
	BEP for setting 2	0.2620	0.0037	0.2620
Inlet pressure	BEP for setting 1	0.0527	0.1119	0.1237
	BEP for setting 2	0.0872	0.1286	0.1554
Discharge	BEP for setting 1	0.0978	0.0016	0.0979
	BEP for setting 2	0.0978	0.0024	0.0978
Speed	BEP for setting 1	0.1321	0.0035	0.1321
	BEP for setting 2	0.1622	0.0016	0.1622
Efficiency	BEP for setting 1	–	–	0.46
	BEP for setting 2	–	–	0.50

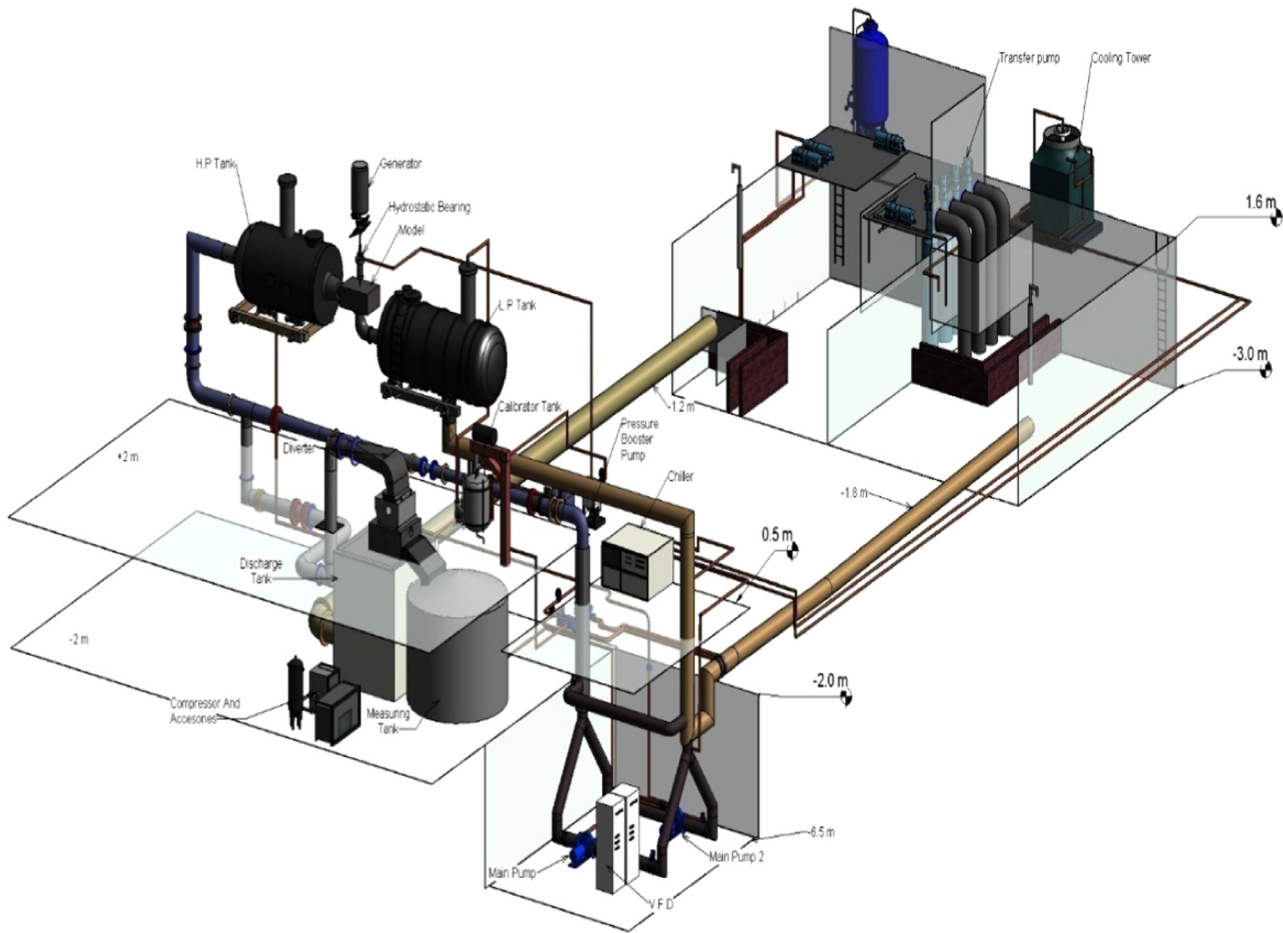


Fig. 1. Three dimensional view of Hydraulic Turbine R&D Laboratory at AHEC, IIT Roorkee.

transducers and output from differential pressure transmitter are logged in SCADA system as shown in Fig. 3.

The calibrated pressure curve and its regression error are shown in Figs. 4 and 5 respectively.

## 2.2. Flow measurement system and calibration

The calibration of the electromagnetic flow meter has been carried in open loop in which water is pumped from a sump having the constant water level and diverted to the measuring tank for a specified period of time through flow diverter using gravimetric approach with flying start- and -stop method as per ISO 5168:2005 [14] and ISO 4158:1980 [5].

In situ calibration chain of flow measurement system is as follows:

### (a) Calibration of balance system

The measuring tank load cell (HBM-RTN) having C3 accuracy class (OMIL R60) are calibrated with the calibrator tank load cell (HBM-S40A) having C3 accuracy class (OMIL R60) then the calibrator tank load cell are calibrated with F2 class knob type weights.

### (b) Calibration of flow meter

The calibration of flow meter was performed using gravimetric method using flying start and stop approach as per ISO 4185:1980 [5].

#### 2.2.1. Calibration of balance system

**2.2.1.1. Standard weights.** The F2 class standard weights duly calibrated from NABL (National Accreditation Board for Testing and Calibration Laboratories) accredited laboratories are used for the

calibration of the calibrator tank load cell.

**2.2.1.2. Calibration of the calibrator tank load cell.** Calibration of the calibrator tank load cell (2 t) is carried out with standard weights up to 1500 kg (72 No- 20 kg, 6 No- 10 kg). The empty weight of the calibrator tank is 490 kg. The output signals from the load cell are logged in the data acquisition system (DAQ-MX410-catman software) having 4 channels.

A curve has been plotted between output signal of load cell (mV) and applied standard weights and as shown in Fig. 6 along with its regression curve as shown in Fig. 7.

**2.2.1.3. Calibration of measuring tank load cell.** Three ring torsion type load cell of 22 t each are placed at the bottom of measuring tank to measure the weight of water collected over a period of diversion time. These load cells are calibrated with a calibrator tank load cell.

A fix calibrated weight of water (about 1300 kg) is transferred from calibrator tank to the measuring tank. The initial and the final output signals (mV) of the load cells (measuring tank and calibrator tank) are logged in data acquisition system (DAQ-MX410 – Catman easy software). The same is repeated until the level of measuring tank reached at maximum. The cumulative corrected weight of water transferred by the calibrator tank is plotted against the primary output signal (mV) of the measuring tank load cell as shown in Fig. 8. Regression error of measuring tank load cell is plotted against applied standard weight as shown in Fig. 9.

#### 2.2.2. The calibration of the electromagnetic flow meter

The calibration of the flow meter is carried out for a discharge range

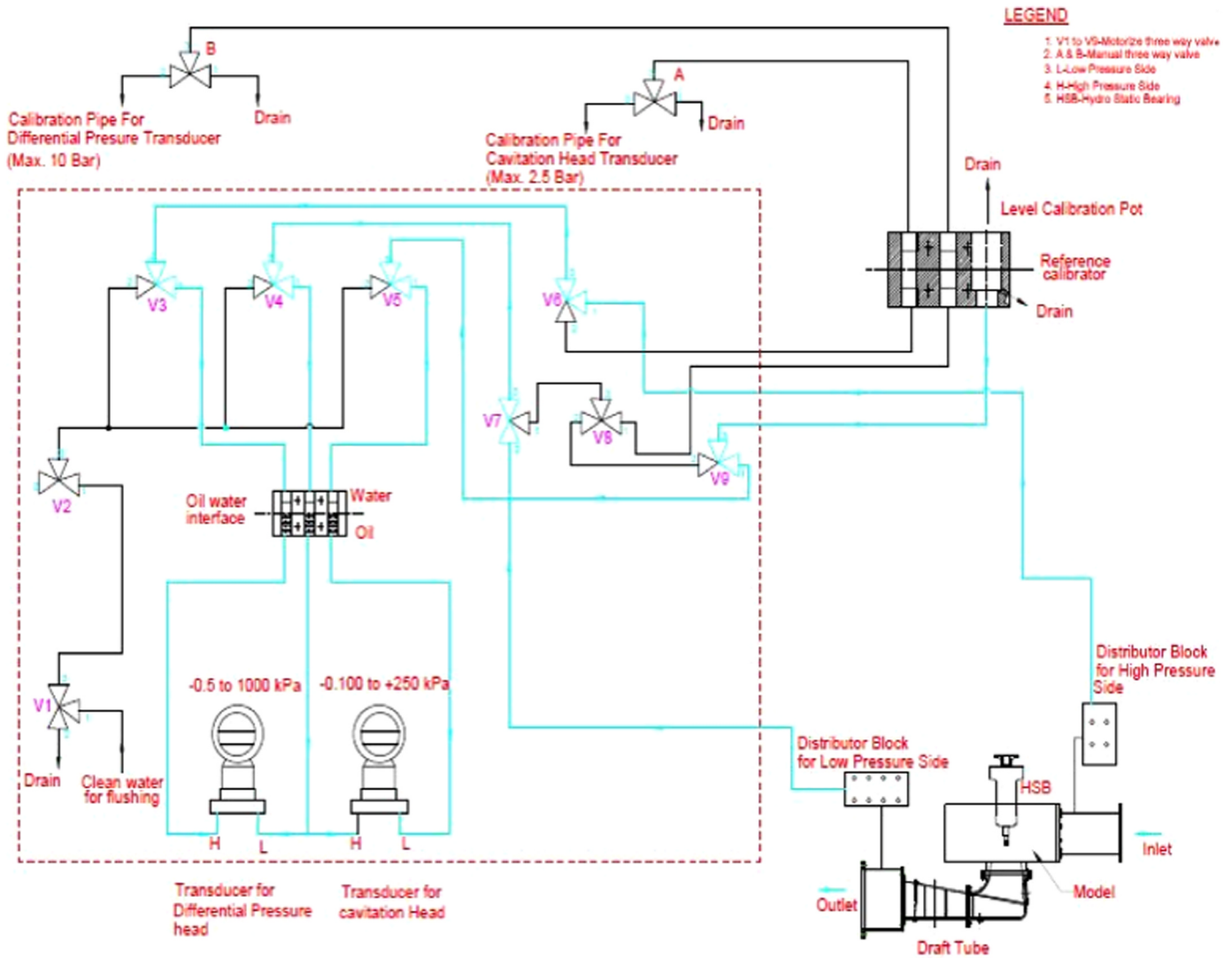


Fig. 2. Set up for differential pressure head measurements.

between 1001/s and 7501/s. the timing error of the diverter system are obtained and used to correct the measured discharge. The water is diverted into the measuring tank for a set period of time until it gets fully filled. Initial and final readings of measuring tank load cells (mV), the initial and the final temperature and diversion time are logged into the SCADA system in order to calculate the discharge. Buoyancy correction is made to the readings of a load cell to take account of the difference between the upward thrust exerted by the atmosphere and the water being weighed. The calibration and the regression curves are plotted in Figs. 10 and 11 respectively.

### 2.3. Torque measurement set up and calibration

The total torque produced by the turbine at any operating point is equal to the sum of calibrated shaft torque, measured by the shaft torque transducer and the friction torque, measured by a the load cell. The shaft torque transducer is fixed on the shaft between the turbine and the generator while the friction torque load cell is connected to the hydrostatic bearing via a lever arm. A calibration arm is connected to the shaft torque transducer. The calibration curve of the shaft torque transducer and the friction torque load cell along with respective regression curve are shown in Figs. 12–15.

The calibration equations of flow and operating parameters such as discharge, shaft torque, friction torque, differential pressure, angular

speed of the runner, measuring tank load cell and calibrator tank load cell are tabulated in Table 3.

### 3. Uncertainty analysis

The uncertainty analysis has been carried for the discharge measurement, torque, net head speed and efficiency. These are as follows:

#### 3.1. Uncertainty in discharge measurement

The uncertainty associated with a discharge measurement is evaluated by combining the uncertainties arising from the sources as per ISO 5168:2005 [14] and JCGM 100:2008 [13]. The combination of all the uncertainties may be made by the root-sum-square method.

Total combined standard uncertainty  $u(Q)_c$  of the discharge measurement is the root sum square of Type A and Type B as per Eq. (8).

$$u(Q)_c = \sqrt{[u(Q)_a]^2 + [u(Q)_b]^2} \tag{8}$$

where  $u(Q)_a$  is the Type A uncertainty of discharge measurement and  $u(Q)_b$  is the Type uncertainty of discharge measurement.

Type B uncertainty in discharge measurement is calculated using Eq. (9).

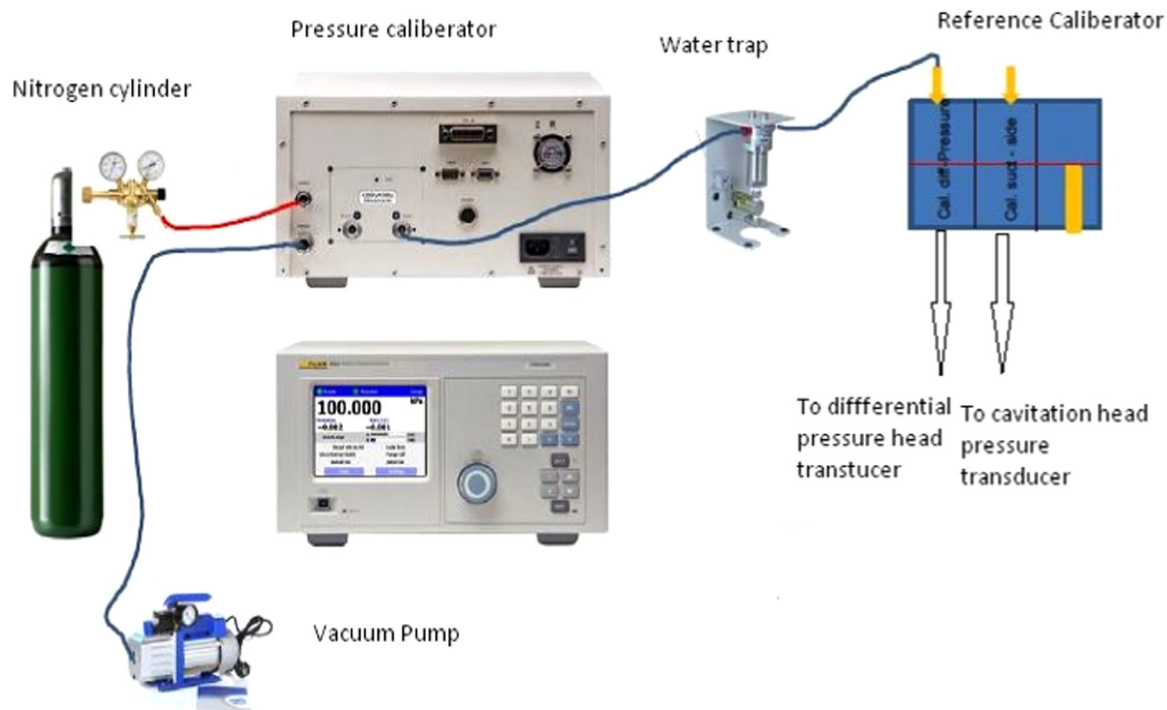


Fig. 3. Calibration of pressure transducers.

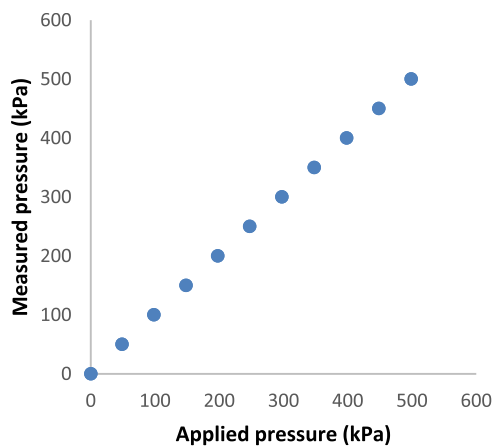


Fig. 4. Calibration of differential pressure head transducer.

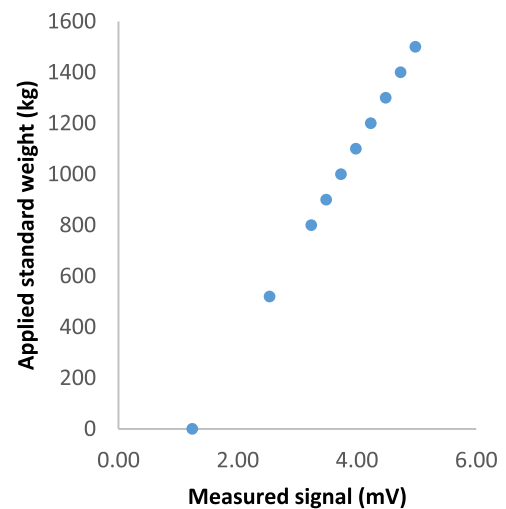


Fig. 6. Calibration curve calibrator tank load cell.

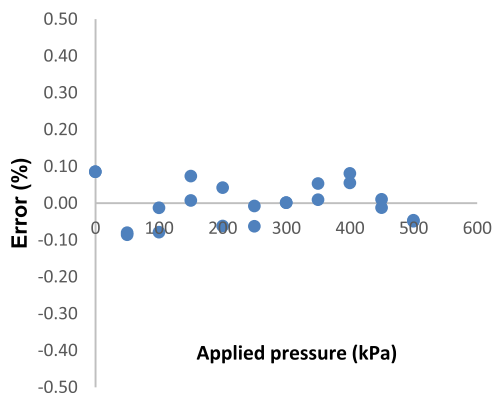


Fig. 5. Regression error of differential pressure head transducer.

$$u(Q)_b = \sqrt{[u(wb)]^2 + [u(p)]^2 + [u(d)]^2 + [u(\epsilon)]^2 + [u(t)]^2} \tag{9}$$

Where  $u(wb)$  uncertainty due to the weighing machine;  $u(p)$  is the uncertainty due to the diverter system;  $u(t)$  is uncertainty due to the timing device;  $u(d)$  uncertainty in the measurement of density.  $u(\epsilon)$  is uncertainty due to buoyancy

In the present study, the buoyancy effect has been calculated in the measuring tank as per Eq. (10) and correction has been made in the total collected weight of water in the measuring tank so that  $u(t)$  in time and  $u(\epsilon)$  is the buoyancy are neglected.

$$M = W^* \left\{ 1 + \rho_{air}^* \left[ \frac{1}{\rho_f} - \frac{1}{\rho_w} \right] \right\} \tag{10}$$

Where  $M$  is the corrected mass, collected in the measuring tank,  $W$  is the balance reading (measured weight by load cell),  $\rho_{air}$  is the density of

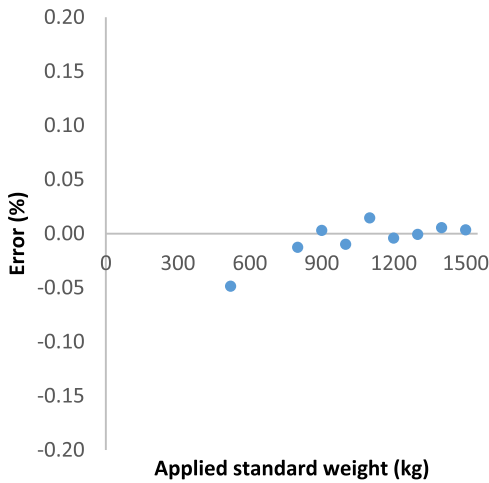


Fig. 7. Regression error of calibrator tank load cell.

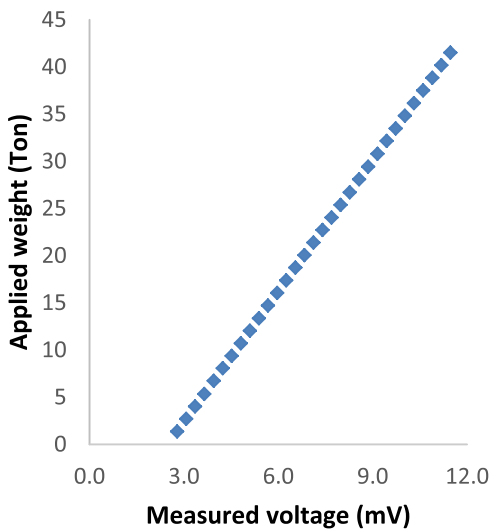


Fig. 8. Calibration curve of measuring tank load cell.

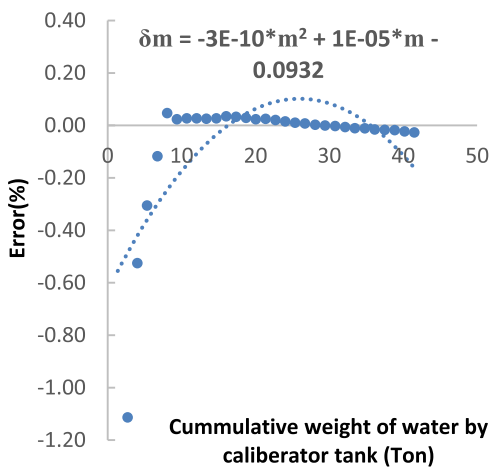


Fig. 9. Regression error of measuring tank load cell.

air,  $\rho_f$  is the density of the fluid(water), and  $\rho_w$  is the density of the tank material.

3.1.1. Evaluation of uncertainty in the weighing balance system

The total uncertainty of the weighing balance system is calculated

by the root sum square of type A and type B error as per Eq. (11)

$$u(wb)_c = \sqrt{[u(wb)_a]^2 + [u(wb)_b]^2} \tag{11}$$

where,  $u(wb)_c$  is combined uncertainty of the weighing balance system;  $u(wb)_a$  and  $u(wb)_b$  is uncertainty type A and type B respectively. In present setup, F2 class weight, calibrator tank and measuring tank constitute the weighing balance system. For evaluation of type A uncertainty of weighing balance system, the standard deviation of the distribution of points about the best-fit curve (shown in Fig. 9) is calculated with 95% confidence limits of the distribution determined using Student's t-table. This value of confidence limits is multiplied by square root of two (since the determination of the mass of water collected in measuring tank during a diversion is obtained from the difference between two weighing) as per ISO 4185:1980 [5]. Type A uncertainty of weighing balance system are found as  $\pm 0.0275\%$ .

Type B uncertainty of measuring tank load cell is calculated using Eqs. (12) and (13).

$$\delta m = -3E - 10*m2 + 1E - 05*m - 0.0932 \tag{12}$$

$$\delta(\Delta m) = \delta m_2 - \delta m_1 \tag{13}$$

Where,  $\delta m_1$ -Error in mass determination of water in measuring tank before diversion;  $\delta m_2$ - Error in mass determination of water in measuring tank after diversion;  $\delta(\Delta m)$ -Uncertainty in mass of water collected in measuring tank

Type B uncertainty of the weighing balance is calculated as per Table 4.

The total standard uncertainty of the weighing balance is calculated as  $\pm 0.07528\%$  by Eq. (11) and expanded uncertainty of weighing balance system at coverage factor  $k \approx 2$  found as  $\pm 0.1506\%$ .

3.1.2. Evaluation of the uncertainty in the diverter system

The total uncertainty of the weighing (balance) system is calculated by root sum square of type A and type B errors as per Eq. (14)

$$u(p)_c = \sqrt{[u(p)_a]^2 + [[u(p)_b]^2} \tag{14}$$

where  $u(p)_c$  is the combined standard uncertainty of the diverter system;  $u(p)_a$  and  $u(p)_b$  are the type A and type B uncertainties of the diverter system respectively.

3.1.3. Type B uncertainty of the diverter system

The correction on measurement in diversion time is also carried out as per method given in ISO 4185:1980 [5] as shown in Fig. 16. The value obtained from the curve  $\Delta t = 0.0217$  s is adjusted in the total diversion time (66.63521 s).

3.1.4. Type A uncertainty of the diverter system

The repeatability with which the duration of a diversion is measured depends on the repeatability of the movement of the diverter which triggers the timing device and on the accuracy with which the triggering position is set. It is determined experimentally by setting the flow-rate to a steady value and then carried out series of 10 diversions for a fixed diversion period to provide a series of 10 estimations of the flow-rate This exercise is repeated for several different diversion periods and, from the standard deviation of each series of measurements, the 95% confidence limits have been evaluated as per ISO 4185:1980 [5]. During flow calibration minimum diversion time was 30 s as per IEC 60193:1999 [3].

Maximum uncertainty of flow diverter system at 30 s in flow calibration was found as  $\pm 0.0067\%$  shown in Fig. 17.

Type A uncertainty for the diverter system is found as 0.033% and the total standard uncertainty of the diverter system is calculated 0.034066 as per Eq. (14). The expanded uncertainty of weighing (balance) system at the coverage factor  $k \approx 2$  found as  $\pm 0.0681\%$ . Uncertainty budget of the discharge measurement is given in Table 5.

Type B uncertainty in the flow measurement during the calibration

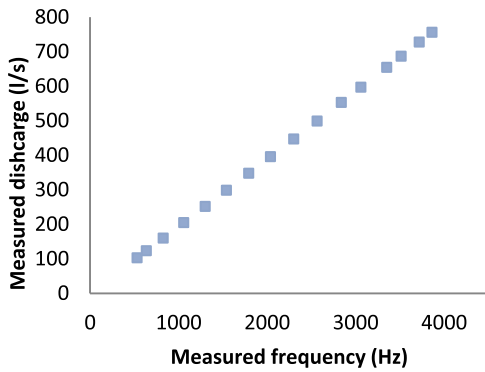


Fig. 10. Flow meter calibration curve.

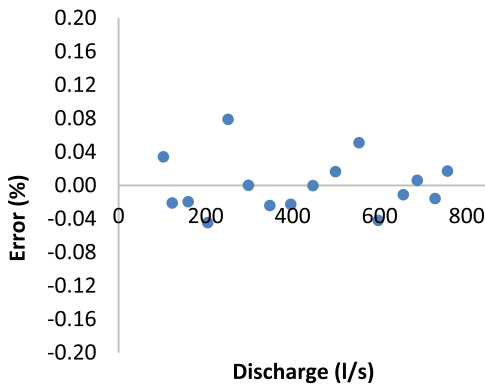


Fig. 11. Regression error of flow meter.

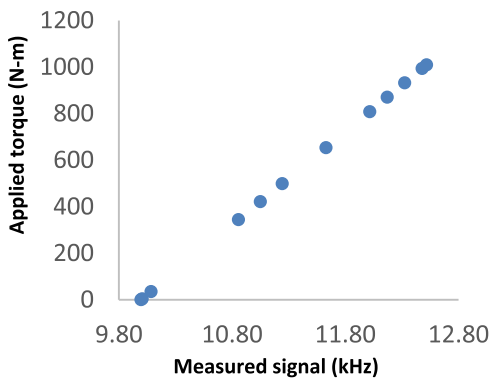


Fig. 12. Shaft torque calibration curve.

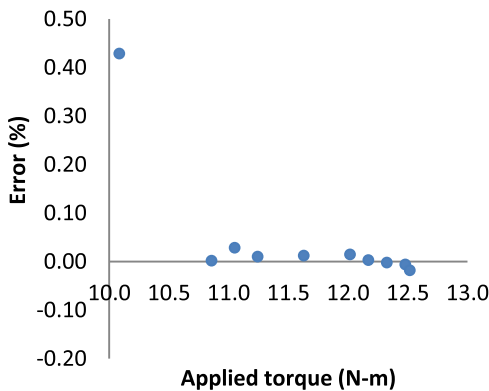


Fig. 13. Shaft torque regression error curve.

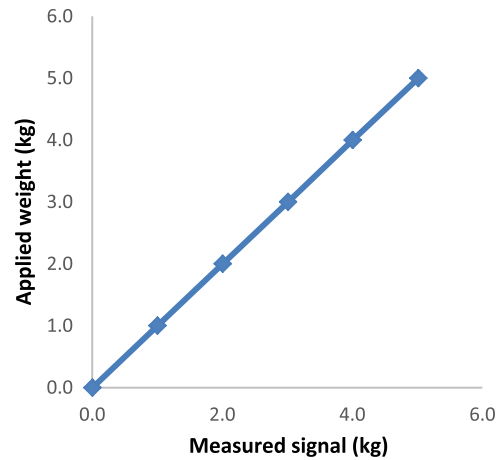


Fig. 14. Friction torque load cell calibration curve.

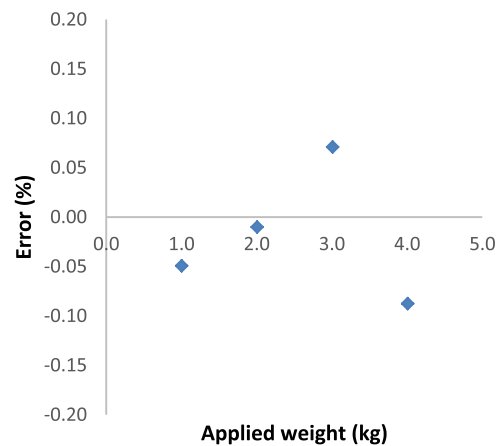


Fig. 15. Friction torque regression error curve.

is calculated and found out as 0.0120% and the total standard and expanded uncertainties in discharge measurement during calibration is calculated as  $\pm 0.0841$  and  $\pm 0.165\%$  for coverage factor  $k \approx 2$  respectively.

During the performance test, at each operating point, the type A uncertainty of flow has been calculated and further used to calculate the total uncertainty of flow. The total uncertainty of flow at each operating point is calculated using Eq. (8) and plotted in Fig. 18. It is observed that at the best efficiency point ( $E_{od} = 0.1723$ ,  $Q_{od} = 0.169$ ) is uncertainty in flow measurement is found a minimum as  $\pm 0.1074\%$ .

### 3.2. Uncertainty in torque measurement

The length of the calibration arm used for shaft torque measurement is measured with micrometer ( $\pm 0.02$  mm) and the uncertainty found out to be  $\pm 0.0012\%$ . The weights used for the calibration have F2 Class accuracy and the total uncertainty of the weights used for calibration is 0.0162%. The length of the calibration arm used for friction torque measurement is measured with a micrometer ( $\pm 0.02$  mm) and the uncertainty found out to be  $\pm 0.00730\%$ . The weights used for the calibration have F2 Class accuracy and total uncertainty of the weights used for calibration is 0.0141%.

The total expanded uncertainty in torque measurement at any operating point is calculated as root sum square of the total shaft torque uncertainty  $u(ST)$  and friction torque uncertainty  $u(FT)$  as per Eq. (15).

$$u(T) = \sqrt{[u(ST)]^2 + [u(FT)]^2} \tag{15}$$

**Table 3**  
Calibration equation of flow and operating parameters.

Parameter	Instrument	Calibration equation
Discharge	Calibrator tank load cell	$(W_{CT})_C = 400.7668*(mV)_{CT} - 495.82$ where, $(W_{CT})_C$ is the calibrated value of weight calibration tank; $(mV)_{CT}$ is the measured voltage by calibrator tank load cell
	Measuring tank load	$(W_{MT})_C = 4622.575*(mV)_{MT} - 11523.86$ where, $(W_{MT})_C$ is the calibrated value of weight by measuring tank; $(mV)_{MT}$ is measured voltage by measuring tank load cell
	Flow meter	$Q_C = 0.0000003*F_F^2 + 0.191448*F_F + 1.318646$ where, $Q_C$ is calibrated discharge; $F_F$ is the frequency obtained from flow meter in kHz
Torque	Shaft torque transducer	$ST_C = 400.1276*(F_{ST}) - 4000.0024$ where, $ST_C$ is the calibrated value of shaft torque; $F_{ST}$ is the frequency obtained from shaft torque sensor
	Friction torque load cell	$W_C = 2.65646*W_M - 4000.0024$ where, $W_C$ is the calibrated friction load weight; $W_M$ is the measured friction weight
Differential Pressure	Differential pressure transducer	$P_C = 1.0028822*(P_M) - 0.26226$ where, $P_C$ is the calibrated differential pressure; $P_M$ is the measured pressure from differential pressure
Speed	Speed sensor	$(RPM)_C = 1.00016*(RPM_M) - 0.02284$ where, $(RPM)_C$ is the calibrated speed of turbine; $(RPM_M)$ is the measured value by speed sensor

**Table 4**  
Type B uncertainty of the weighing balance.

S. no.	Uncertainty component	Standard uncertainty (%)	Total type B standard uncertainty in weighing balance $u(wb)_b$
1.	Standard Weights	$\pm 0.00456$	$\pm 0.0701\%$
2.	Calibrator tank load cell	$\pm 0.050$	
3.	Measuring tank load cell	$\pm 0.0489$	

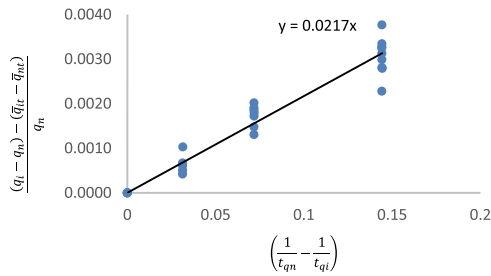


**Fig. 16.** Diversion time correction.

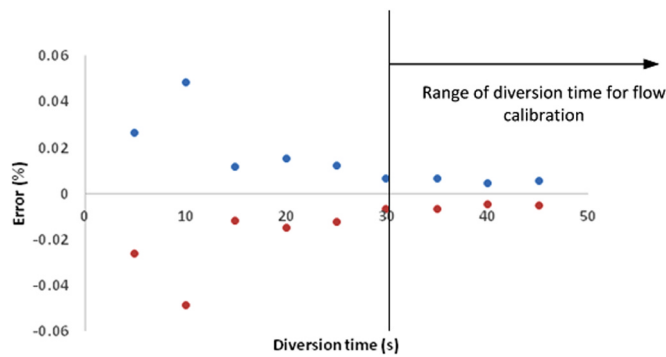


**Fig. 17.** Random error in diverter time.

The combined uncertainties of the Shaft torque and friction torque are as below:

$$u(ST)_c = \sqrt{[u(ST)_a]^2 + [u(ST)_b]^2 + [u(ST)_{reg.}]^2} \tag{16}$$

The shaft torque standard uncertainty is the combined uncertainty of the weights used for the calibration  $u(w, st)$  measurement of calibration arm .regression error at nearest operating point  $u(ST)_{reg.}$  and

$u(ST)_a$  is type A uncertainty of shaft torque measurement during calibration

$$u(ST)_b = \sqrt{[u(w, st)]^2 + [u(cal. arm)]^2} \tag{17}$$

The standard uncertainty in friction torque measurement is also calculated in same manner as per Eq. (17)

$$u(FT)_c = \sqrt{[u(FT)_a]^2 + [u(w, st)]^2 + [u(cal. arm)]^2 + [u(FT)_{reg.}]^2} \tag{18}$$

The standard uncertainties in shaft torque and friction torque during the calibration is calculated as 0.0164% and 0.0518% using Eqs. (16) and (18) respectively. Standard and expanded uncertainties in torque measurement during calibration are calculated as  $\pm 0.0543\%$  and  $\pm 0.107\%$  for coverage factor  $k \approx 2$  corresponding to 95% confidence limit, respectively.

The total uncertainty in torque measurement at 16 different operating points is calculated and plotted in Fig. 16. It is observed that at the fixed  $E_{\omega d}$ , torque uncertainty is the minimum at best efficiency point and found out as  $\pm 0.1683\%$ . It is also observed that at fixed  $E_{\omega d}$  torque uncertainty increase at off design points (part load and overload). There is also an interesting trend which are observed from the Fig. 17 that at  $E_{\omega d} = 0.1421$ , torque uncertainty is minimum at each discharge coefficient ( $Q_{\omega d} = 0.18679, 0.17177, 0.15437$  and  $0.11943$ ) (Fig. 19).

### 3.3. Uncertainty in net head measurement

The differential pressure transmitter is calibrated with a pressure calibrator having an uncertainty of  $\pm 0.011\%$ . In head measurement the source of uncertainty components are the differential head  $\frac{(\Delta p)}{\rho * g}$  and the dynamic head  $\frac{(v_1^2 - v_2^2)}{2 * g}$ . Type B uncertainty in net head measurement is calculated by obtaining the uncertainty of differential head, the uncertainty of inlet velocity  $v_1$  and outlet velocity  $v_2$  measurement. Total type B uncertainty in net head measurement is given in Eq. (19)

**Table 5**  
Uncertainty budget of discharge measurement.

Source of uncertainty	Estimates ( $X_i$ )	Unit	Limits (%)	Probability distribution type A or B	Standard uncertainty ( $U_i$ )	Sensitivity coefficient ( $C_i$ )	Uncertainty contribution $U_i(y) = C_i * U_i$ (%)	Degree of freedom
Weighing (balance) system $u(wb)$	37,950.71	kg	0.1506	Type B normal	0.0753	1	0.0753	$\infty$
Timing device $u(t)$	64.2748	sec	Negligible	Type B Rectangular	0.0000	1	0.0000	$\infty$
Diverter system $u(p)$	64.2748	sec	0.0681	Type B normal	0.0341	1	0.0341	$\infty$
Density $u(d)$	996.4	kg/m <sup>3</sup>	0.0200	Type B Rectangular	0.0100	1	0.0100	$\infty$
Q	0.592573	m <sup>2</sup> /s	Total Type B		$u(Q)_b$	0.0832	$\infty$	
Repeatability $u(Q)_a$	3231.9	Hz		Type A Normal	0.067	1	0.0113	299
Regression error $u(Q)_{reg.}$	Type A Normal				0.0040	1	0.0040	15
Total type A $u(Q)_a$ (%)							0.0120	
Total standard uncertainty with regression error $u(Q)_c$ (%)							0.0841	
<b>Expanded uncertainty (<math>k = 2</math>) <math>u(Q)</math> (%)</b>							<b><math>\pm 0.165</math></b>	

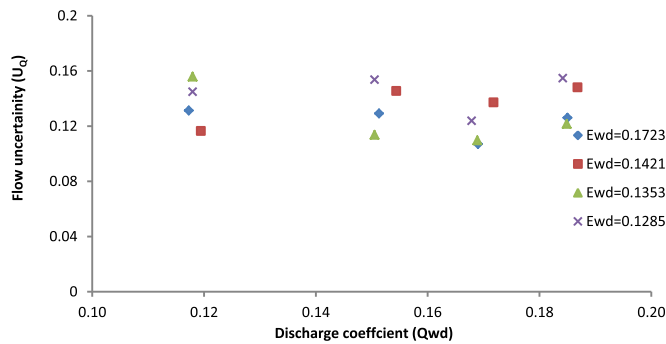


Fig. 18. Total uncertainty in flow measurement at different operating points.

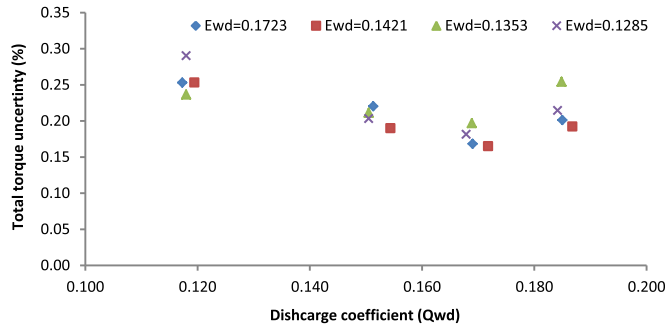


Fig. 19. Total uncertainty in torque measurement at different operating points.

$$u(H) = \pm \frac{\sqrt{\left(\frac{U_{\Delta p}}{\rho * g}\right)^2 + \left(\frac{U_{v1}^2}{2g}\right)^2 + \left(\frac{U_{v2}^2}{2g}\right)^2}}{\frac{(\Delta p)}{\rho * g} + \frac{(v_1^2 - v_2^2)}{2 * g}} \quad (19)$$

Type A and Type B uncertainties in the net head measurement in calibration are found as 0.001% and 0.01194% respectively. So the total standard and the expanded uncertainty in the head measurement system are found as 0.012% and 0.024% for a coverage factor  $k \approx 2$  corresponding to 95% confidence limit, respectively.

During the performance test, at each operating point, the type A uncertainty of net head has been calculated and further used to calculate the total uncertainty of net head measurement. Uncertainty in net head measurement at 16 different operating points is evaluated with 95% confidence limits of the distribution. Total uncertainty in head measurement at each operating point is plotted as shown in Fig. 18.

From the Fig. 20, it is observed that the magnitude of total uncertainty in the net head measurement is very low at each operating point.

### 3.4. Uncertainty in speed measurement

The speed sensor is calibrated with a stroboscope (Drello 3020) having an uncertainty of  $\pm 0.001\%$ . At each operating point the regression error (nearest calibration point) during calibration in speed calibration was obtained from the calibration curve. The standard and expanded uncertainties in speed measurement were calculated as  $\pm 0.004149\%$  and  $0.008298\%$  for coverage factor  $k \approx 2$  corresponding to 95% confidence limit, respectively.

Performance test were carried out at 1000 rpm and type A error at each operating point is calculated with 95% confidence limits of the normal distribution. Total uncertainty in speed at each operating point is plotted as shown in Fig. 21.

### 3.5. Uncertainty in efficiency measurement

The efficiency at different operating points is evaluated from the calibrated values of different parameters (discharge, net head, torque and speed) and plotted in Fig. 22. From the Fig. 22, it is observed that the efficiency at the best efficiency point ( $E_{od} = 0.1723$ ,  $Q_{od} = 0.169$ ) is maximum and off design points efficiency goes down.

The total uncertainty in efficiency measurement during the performance test at any operating point is estimated statistically by introducing the uncertainty of each of the measured quantities as

$$u(\eta) = \sqrt{[u(Q)]^2 + [u(T)]^2 + [u(H)]^2 + [u(d)]^2 + [u(\omega)]^2} \quad (20)$$

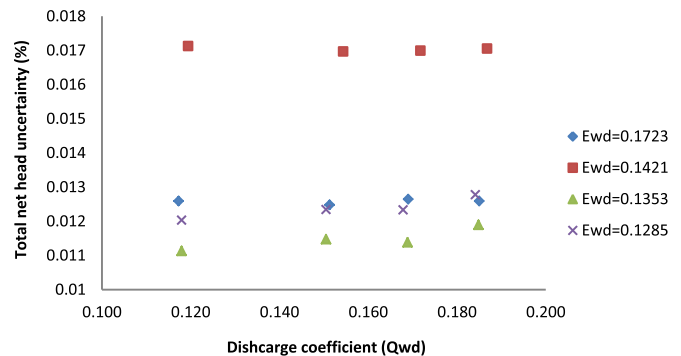


Fig. 20. Total uncertainty in net head measurement at different operating points.

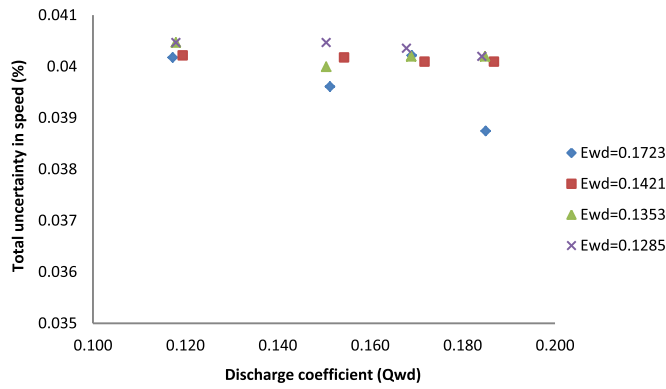


Fig. 21. Total uncertainty in speed at different operating points.

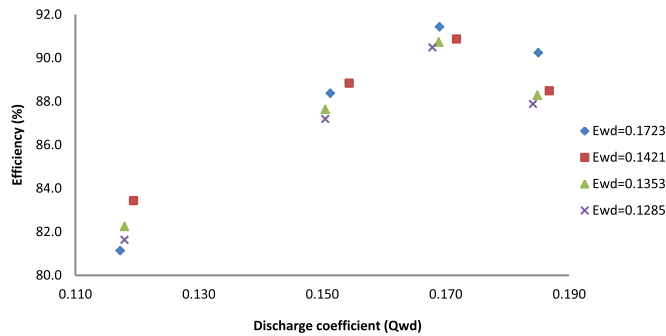


Fig. 22. Evaluation of efficiency at different operating points.

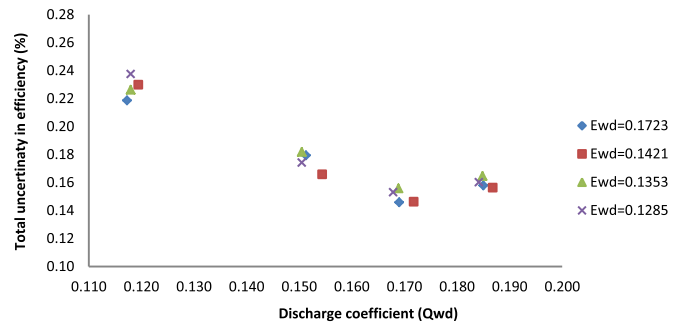


Fig. 23. Total uncertainty in efficiency measurement.

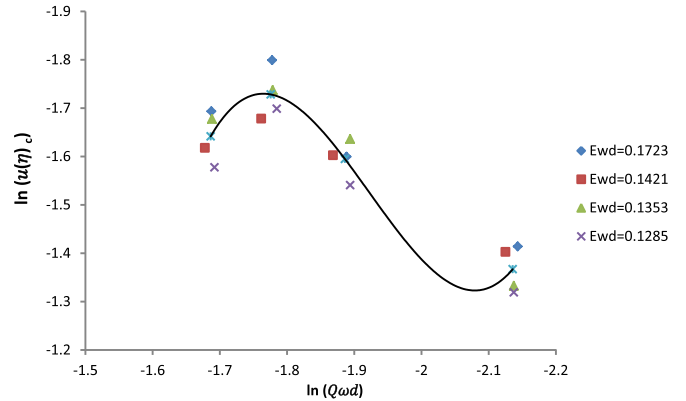


Fig. 24. Variation of uncertainty in efficiency measurement ( $u(\eta)_c$ ) with different discharge coefficient  $Q_{wd}$ .

- $u(Q)$  – is uncertainty in discharge measurement
- $u(T)$  – is uncertainty in torque measurement
- $u(H)$  – is uncertainty in head measurement
- $u(d)$  – is uncertainty in density measurement
- $u(\omega)$  – is uncertainty in angular speed measurement of model turbine

The overall uncertainty is given in the Table 6.

The total standard uncertainty in efficiency measurement  $u(\eta)_c$  at different operating points is shown in Fig. 23. It is observed from the Fig. 23 that the uncertainty in efficiency measurement is minimum as  $\pm 0.1411\%$  at the best efficiency point ( $E_{od} = 0.1723$ ,  $Q_{od} = 0.169$ ) and off design points (part load and overload) uncertainty increases. It can be also observed that at constant  $E_{od}$ , the uncertainty in efficiency measurement at part load operating points increases with a faster rate compared with overload point.

From the graph it is observed that the variation of uncertainty in the efficiency measurement ( $u(\eta)_c$ ) seems to be influenced slightly by

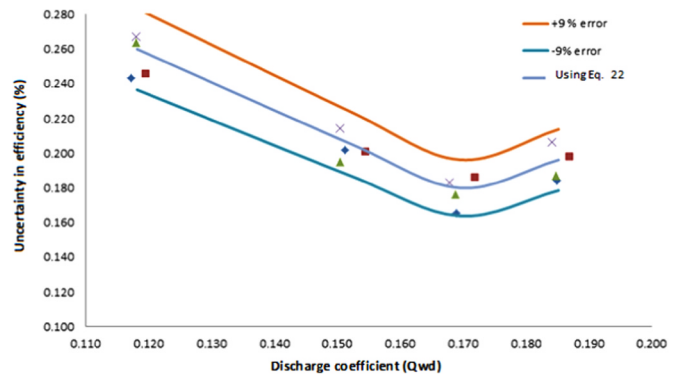


Fig. 25. Comparison of experimental and predicted uncertainty in efficiency measurement ( $u(\eta)_c$ ) due to discharge coefficient  $Q_{od}$ .

Table 6  
Uncertainty budget for efficiency measurement.

Source of uncertainty	Estimates ( $X_i$ )	Unit	Limit (%)	Probability distribution type A or B	Standard uncertainty ( $U_i$ )	Sensitivity coefficient ( $C_i$ )	Uncertainty contribution $U_i(y) = C_i * U_i$ (%)	Degree of freedom
Discharge $u(Q)$	0.57159	$m^2/s$	0.1650	Type B normal	0.0825	1	0.0825	$\infty$
Torque $u(T)$	957.59	N-m	0.1070	Type B normal	0.0535	1	0.0535	$\infty$
Net head $u(H)$	19.57	m	0.0240	Type B normal	0.0120	1	0.0120	$\infty$
Speed $u(\omega)$	999.63	$kg/m^2$	0.0083	Type B normal	0.0041	1	0.0041	$\infty$
Density $u(d)$	999.96	1/min	0.0200	Type B normal	0.0100	1	0.0100	$\infty$
Efficiency $u(\eta)_a$	91.535	%	<b>Type B</b>				0.0996	$\infty$
Repeatability $u(\eta)_a$	91.535	%	0.0998	Type A Normal	0.0998	1	0.0998	299
Total Type A $u(\eta)_a$							<b>0.00998%</b>	
Total Type B $u(\eta)_b$							<b>0.0996%</b>	
Total standard uncertainty $u(\eta)_c$							$\pm 0.1411\%$	
Expanded uncertainty ( $k = 2$ ) $u(\eta)$							$\pm 0.2765\%$	

energy coefficient ( $E_{\text{wd}}$ ). An empirical relationship of total uncertainty in efficiency measurement ( $u(\eta)_c$ ) due to discharge coefficient  $Q_{\text{wd}}$  was developed using the regression analysis of the experimental data is expressed as given in Eq. (21)

$$(u(\eta)_c) = e^{c_0} * Q_{\text{wd}}^{c_1} * e^{c_2(\ln Q_{\text{wd}})^2} * e^{c_3(\ln Q_{\text{wd}})^3} \text{ for } 0.11815 \leq Q_{\text{wd}} \leq 0.1852 \quad (21)$$

The average values of uncertainty in the efficiency measurement ( $u(\eta)_c$ ) are plotted against different discharge coefficient  $Q_{\text{wd}}$  on a log-log scale as shown in Fig. 24.

Thus the uncertainty in efficiency measurement ( $u(\eta)_c$ ) can be expressed as shown in Eq. (22)

$$y = e^{180.27} * Q_{\text{wd}}^{287.64} * e^{150.67 * (\ln Q_{\text{wd}})^2} * e^{26.13 * (\ln Q_{\text{wd}})^3} \quad (22)$$

An error of  $\pm 9\%$  in the Eq. (21) for the estimation of uncertainty in the efficiency measurement ( $u(\eta)_c$ ) for the experimental data of the present investigation as shown in Fig. 25. Eq. (22) can be used to predict the uncertainty in efficiency measurement ( $u(\eta)_c$ ) due to the discharge coefficient for  $0.11815 \leq Q_{\text{wd}} \leq 0.1852$  and an energy coefficient range of  $0.1285 \leq E_{\text{wd}} \leq 0.1723$ .

#### 4. Conclusions

The in-situ calibration of flow and operating parameters viz. discharge, head, speed and torque has been performed. Efficiency and total uncertainties in efficiency, discharge, head, speed and torque are evaluated at different operating points. It was observed that at the best efficiency point the uncertainty in efficiency measurement is minimum as  $\pm 0.1411\%$ . An interesting trend has been observed that at each energy coefficient ( $E_{\text{wd}}$ ), the uncertainty in efficiency measurement at part load point (PL<sub>1</sub>) is more compared to overload point (OL). A correlation with  $\pm 9\%$  error is also developed to predict uncertainty in efficiency measurement in operating range of turbine.

#### Acknowledgement

Financial support for the doctoral fellowship to author study was provided by the Ministry of New and Renewable Energy, Govt. of India is thankfully acknowledged.

#### References

- [1] V. Fabre, A. Duparchy, F. Andre, P. Larroze, State of the art hydraulic turbine model test, in: Proceedings of the 28th IAHR symposium on Hydraulic Machinery and Systems, Grenoble, France, 2016.
- [2] G. Johnson, C.P. Kittredge, R.A. Newey, J.S. Hunter, Evaluation of measurement uncertainties in performance testing of hydraulic turbines and pump/turbines, *J. Eng. Power* (1975) 145–152.
- [3] IEC 60193: 1999-11. Hydraulic turbines, storage pumps and pump-turbines – Model acceptance tests. International Electro-technical Commission, Geneva.
- [4] ASME PTC-18, Hydraulic Turbines and Pump-Turbines, Performance Test Codes, ASME, New York, 2011, p. 92.
- [5] ISO 4185, Measurement of Liquid Flow in Closed Conduits – Weighing Method, International organization for Standardization, Switzerland, 1980, p. 26.
- [6] R.A. Stople, Testing Efficiency and Characteristics of a Kaplan-Type Small Turbine (Project Thesis), Norwegian University of Science and Technology, 2011.
- [7] L. Fjaervold, Improvements of a Kaplan Type Small Turbine (Master Thesis), Norwegian University of Science and Technology, 2011.
- [8] C. Kvangeres, Investigation of Small Hydro Turbine (Master Thesis), Norwegian University of Science and Technology, 2012.
- [9] C. Trivedi, M.J. Cervantes, B. Gandhi, O.G. Dahlhaug, Experimental and numerical studies for a high head Francis turbine at several operating points, *ASME J. Fluids Eng.* (2013) 135.
- [10] <<https://www.ntnu.edu/nvks/experimental-study>>, (Accessed 7 July 2017).
- [11] U. Andersson, M.J. Cervantes, Phase resolved velocity measurements at the draft tube cone of the turbine-99 test case, in: Proceedings of the IAHR 24th Symposium on Hydraulic Machinery and Systems, 2008.
- [12] P. Guo, Z. Wang, L. Sun, X. Luo, Characteristic analysis of the efficiency hill chart of Francis turbine for different water heads, *Adv. Mech. Eng.* 9 (2) (2017) 1–8.
- [13] JCGM 100:2008, Evaluation of measurement data – guide to the expression of uncertainty in measurement, p. 134.
- [14] ISO 5168, Measurement of Fluid Flow – Procedure for the Evaluation of Uncertainties, International organization for standardization, Switzerland, 2005, p. 71.